*OCEANOLOGY, 2025, Vol. 65, No. 1, pp. 67–82*

MARINE CHEMISTRY

# ORIGIN OF HYDROCARBONS IN HOLOCENE SEDIMENTS OF THE NORDIK SEAS AND BARENTS SEA

**© 2025 I. A. Nemirovskaya*, and A. V. Medvedeva**

*Shirshov Institute of Oceanology, RAS, Moscow, Russia*

**e-mail: nemir@ocean.ru*

Received April 18, 2024
Revised June 10, 2024
Accepted October 03, 2024

**Abstract.** The concentrations and composition of hydrocarbons (aliphatic – AHCs and polycyclic aromatic hydrocarbons – PAHs) were determined using molecular markers in Holocene sediments of the Nordik Seas and the Barents Sea (cruise 84 of the R/V *Akademik Mstislav Keldysh*, 2021). A wide range of concentrations in surface bottom sediments has been established: $C_{org}$ (0.25–2.71%), AHCs (7–182 μg/g) and PAHs (0–1918 ng/g). The distribution of hydrocarbons is determined mainly by the processes occurring in the sedimentary strata (changes in Eh and fluid flows), and to a lesser extent by the lithotype of sediments. At the same time, the formation of autochthonous homologues is observed in the composition of alkanes, and in the composition of PAHs – naphthalenes.

**Keywords:** *aliphatic and polycyclic aromatic hydrocarbons, Nordik Seas, Barents Sea, bottom sediments, fluid flows*

**DOI:** 10.31857/S00301574250106e8

## INTRODUCTION

The ubiquity of hydrocarbons (HC) in water bodies, their active participation in physicochemical and biochemical processes, interaction with aquatic organisms, as well as the inflow of petroleum HC from various sources leads to difficulties in determining their origin [7, 17, 41–43]. According to the remote sensing data obtained by Sentinel-1A and Sentinel-1B radar satellites, the presence of oil films on the sea surface may indicate not only an anthropogenic but also a natural source of their input [8, 26].

During the inventory of oil HC sources in the World Ocean, it was concluded that their main share (46% of the sum of 1300 thousand tons) comes as a result of natural deposition on the bottom from the underlying sedimentary strata [17]. The Barents and Norwegian Seas are among the largest oil and gas bearing basins of the Arctic [3], on the coasts of which, economic activity is actively carried out [11, 20]. Urbanized territories, ports, oil loading terminals are located here and, accordingly, pollutants coming from the shore and formed in the sea itself as a result of human economic activity are concentrated [5, 18].

For reliable assessment of anthropogenic HC in the marine environment it is necessary to establish the locations and extent of natural oil spills in the sea, and to assess the natural hydrocarbon background on which this pollution is superimposed. Therefore, the study of HC becomes nowadays a particularly relevant and necessary stage in the environmental monitoring of the Arctic seas for subsequent geo-ecological control during geological exploration and mining [7, 12, 17, 18, 31]. In addition, obtaining reliable estimates of HC characteristics and their role in the ocean carbon balance is one of the important tasks in creating a system for monitoring climate change [13].

The purpose of this study is to determine the concentrations and composition of HCs (aliphatic hydrocarbons and polycyclic aromatic hydrocarbons) in bottom sediments of the Norwegian-Greenland Basin and the Barents Sea in order to establish their origin.

In August 2021. during the 84th cruise of the R/V "Akademik Mstislav Keldysh" the following areas were covered by the research [4, 10]: The deep-water part of the Greenland Basin, the northern part of the East Greenland Ridge, the near-breakup zone near the junction of the Mona and Knipovich Ridges, the western and northwestern extremities of the Svalbard continental shelf (Westnes Ridge, Sofia Basin and the Hinlopen Trog), Fram Strait, the area of the Orli

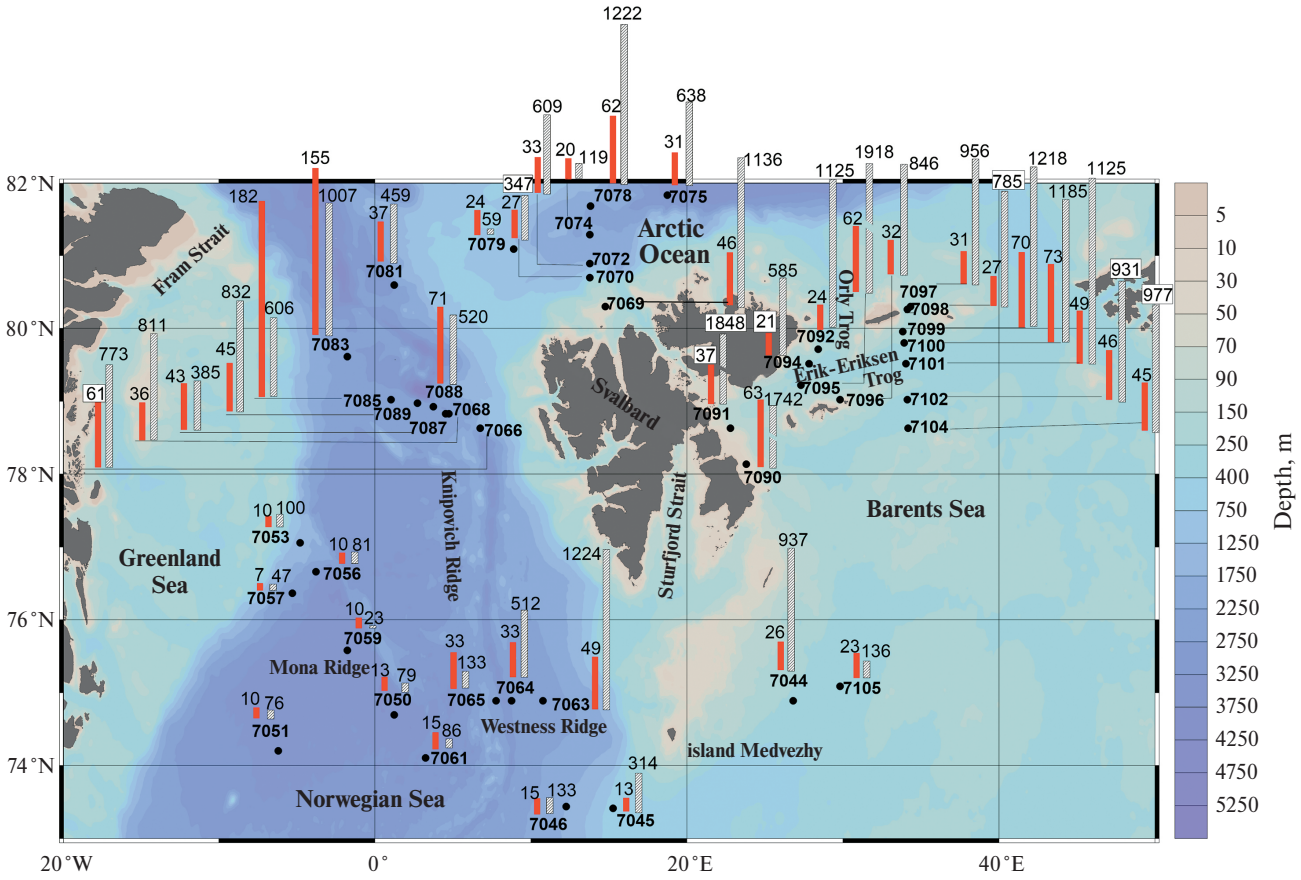


**Fig. 1.** Sampling map and distribution of PAHs (red columns, μg/g) and PAHs (shaded columns, ng/g) in the surface layer of bottom sediments during the 84th cruise of the R/V "Akademik Mstislav Keldysh".

Trough with the intersection of the Erik-Eriksen Trog and the central part of the Barents Sea (Fig. 1).

## MATERIALS AND METHODS

Bottom sediment samples were collected using an Ocean-50 dredge and undisturbed sediment columns collected using a multicorer (Mini Muc K/MT 410, KUM, Germany), which were divided into layers and frozen until analysis in the laboratory. The thickness of the uncovered sediment layer varied from 1 cm (dredge) to 32 cm (multicorer). Sediment samples were dried at 50° C, and HC was ultrasonically extracted from the sediment fraction < 0.25 мм with methylene chloride (all solvents used were qualified o.s.h.).

The concentration of PAHs was determined by infrared method on an IRAffinity-1 spectrophoto meter manufactured by Shimadzu, Japan; alkanes – by gas chromatographic method on a Crystal-Lux 4000-M chromatograph (Russia); PAHs concentration – by fluorimetry [15] on a "Trilogy" device manufactured by Turner (USA), and their composition – by high-performance liquid chromatography (HPLC) on a Shimadzu LC-20 device, Japan: column – "Envirosep PP", at thermostat temperature 40°C in gradient mode from 50% to 90% volume fraction of acetonitrile in water, eluent flow rate – 1 $cm^3$/min. A fluorescence detector "RF-20A" with programmable excitation and detection wavelengths was used. The calculation was performed using the software "LC Solution". The instrument was calibrated using individual PAHs and their mixtures produced by "Supelco" (Merck, Germany). As a result, priority polyarenes recommended in the study of pollution of marine objects by EPA (Environmental Pollution Agency) were identified [30]: NAF-naphthalene, MeNAF – 1-methylnaphthalene, 2-MeNAF – 2-methylnaphthalene, ACNF – acenaphthene, FLR – fluorene, FEN – phenanthrene, ANTR – anthracene, FLT – fluoranthene, PR – pyrene, BaA – benz(a)anthracene, CHR – chrysene, BEP – benz(e)pyrene, BbF – benz(b)fluoranthene, BkF – benz(k)fluoranthene, BaP – benz(a)pyrene, DBA – dibenz(a,h)anthracene, BPL – benz(g,h,i)perylene, IND – indeno[1,2,3-c,d]pyrene, PR – perylene.

Organic carbon ($C_{org}$) in bottom sediments was determined by the dry combustion method on a TOC-L instrument (Shimadzu, Japan). The coefficient 0.86 was used to convert HC concentrations to $C_{org}$ concentrations [7].

## RESULTS AND DISCUSSION

In surface bottom sediments, the content of AHCs varied from 7 μg/g at station 7067 offshore Greenland to 182 μg/g at station 7085 in Fram Strait (Fig. 1), and $C_{org}$ from 0.25% at station 7053 (also offshore Greenland) to 2.71% at station 7105 east of Medvezhy Island (Table 1).

The concentrations of $C_{org}$ and AHCs in the Fram Strait sediments also varied in a wide range: 0.81–1.87% and 20–182 μg/g, respectively (Table 1). While on average the fraction of AHCs in the $C_{org}$ composition of all studied bottom sediments was 0.23%, in Fram Strait it increased at stations 7083 and 7085 up to 0.93%, which is atypical for the background areas of the Arctic lying outside the active anthropogenic activity [7]. The concentrations of AHCs at stations 7083 and 7085 were close (155 and 182 μg/g). Nevertheless, the content of alkanes (3.9 and 0.1 μg/g) as well as their composition differed greatly (Fig. 2a). Indeed, at Station 7085, the composition of alkanes was dominated in the low molecular weight region by the n–$C_{16}$ homologue, which is of microbial origin [32, 34]. As a result, the ratio of low-molecular to high-molecular alkanes: $L/H = \sum(C_{12(-24)})/\sum(C_{(25-35)})$ increased to 2.0 (Table 2). In contrast, the sediments of st. 7083 were dominated by high-molecular-weight odd terrigenous homologs, and the L/H value decreased to 0.37. The CPI value (the ratio of odd to even homologs at $C > 25$) in the sediments of these stations was the highest (4.10–6.37) compared to the other studied areas. While at station 7083 the contents of pristan and phytane were practically equal (Pr/Pf = 0.99), at station 7085 phytane dominated (Pr/Pf= 0.49). The latter, as well as other markers indicate the different nature of alkanes.

The section along the Vestnes Ridge west of Svalbard was located in the area of the most known active methane seafloor venting in the Arctic [38, 39]. The maximum content of $C_{org}$ (2.25%), AHCs (49 μg/g), and PAHs (1224 ng/g) in this section is confined to station 7063, located in the fjord cone zone (Horsunn Bay) at a depth of 319 m. The surface layer (0–1 cm) of the sediment contained fragments of bivalve shells, a significant amount of chemosymbiotrophic benthos – polychaetes of the family *Siboglinidae* and their tubes. In the underlying sediment column (deeper than 1 cm), the content of AHCs increased unevenly in the transition from oxidized to reduced layers (Fig. 3). Their highest concentrations were found at the horizon of 10–11 cm (82 μg/g) and 15–16 cm (81 μg/g), but in the lower layers of the column (22–24 cm) their content also remained rather high (49–66 μg/g), as well as the $C_{org}$ content (2.01–2.08%). In these layers, the growth of AHCs concentrations was due to the degradation of organic matter, as the $C_{org}$ content decreased.

The composition of alkanes indicated intensive autochthonous processes occurring in the sedimentary column at station 7063 (Fig. 4): the L/H ratio increased with burial depth from 0.95 to 1.85 (Table 2), reaching a maximum at the 23–24 cm horizon, as did the pristane/phytane ratio (0.85).

A different distribution in the sediment column at station 7063 was observed for PAHs (Fig. 3). Their concentrations sharply decreased in the surface horizons (from 1224 ng/g to analytical zero), and in the 7–8 cm layer, they increased reaching 75 ng/g at the hill. 10–11 cm. Polyarenes were absent in the lower

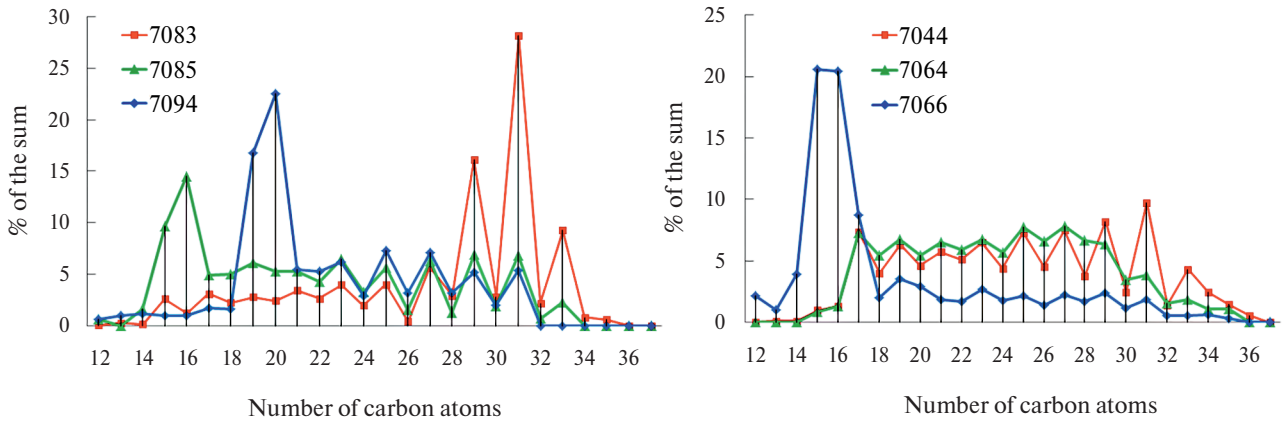


**Fig. 2.** Composition of alkanes in the surface layer of bottom sediments at selected stations.

**Table 1.** Characterization of the surface layer of bottom sediments of the Norwegian and Barents Seas in different years of study

| Neighborhood | *n** | AHCs, μg/g | | PAH**, ng/g | | $C_{org}$, % | | Moisture, % | |
|---|---|---|---|---|---|---|---|---|---|
| | | interval | average | interval | average | interval | average | interval | average |
| August 2021 г. | | | | | | | | | |
| All neighborhoods | 41 | 7–182 | 42 | 23–1918 | 663 | 0.25–2.41 | 1.56 | 36.8–82.4 | 58.2 |
| Southern part | 12 | 7–61 | 20 | 23–1224 | 235 | 0.25–2.31 | 1.34 | 38.3–66.7 | 50.6 |
| Fram Strait | 13 | 20–182 | 50 | 59–1222 | 635 | 0.81–1.87 | 1.45 | 42.9–82.4 | 61.2 |
| Northeastern part | 16 | 24–73 | 48 | 136–1918 | 1119 | 1.46–2.41 | 1.85 | 48.1–73.6 | 61.8 |
| August-September 2016 г. | | | | | | | | | |
| All neighborhoods | 42 | 3–44 | 14 | Not defined. | Not defined. | 0.07–2.59 | 1.08 | 20.1–69.7 | 45.6 |
| Shtokman landfill | 7 | 9–27 | 15 | Not defined. | Not defined. | 0.67–2.57 | 1.81 | 23.7–69.7 | 53.0 |
| Medvezhinsky Trough | 10 | 6–44 | 17 | Not defined. | Not defined. | 0.25–1.71 | 0.79 | 27.0–58.5 | 40.6 |
| Russian harbor | 7 | 4–22 | 11 | Not defined. | Not defined. | 0.24–1.86 | 0.96 | 27.9–60.0 | 40.1 |
| Svalbard – FJL | 8 | 8–24 | 16 | Not defined. | Not defined. | 0.70–1.47 | 1.21 | 33.2–68.5 | 55.5 |
| July-August 2017 г. | | | | | | | | | |
| All neighborhoods | 48 | 3–57 | 12 | Not defined. | Not defined. | 0.03–2.38 | 1.02 | 17.0–72.1 | 49.5 |
| Western part | 16 | 15–37 | 10 | Not defined. | Not defined. | 0.30–1.69 | 0.65 | 30.4–60.7 | 49.6 |
| Svalbard – FJL | 14 | 4–37 | 13 | Not defined. | Not defined. | 0.72–2.38 | 1.52 | 37.6–72.0 | 54.3 |
| New Earth | 5 | 6–57 | 19 | Not defined. | Not defined. | 0.80–1.66 | 1.19 | 40.5–63.4 | 49.8 |
| Central part | 13 | 4.4–17.2 | 10.8 | Not defined. | Not defined. | 0.03–1.94 | 0.93 | 17.0–63.4 | 49.1 |
| May-June 2019 г. | | | | | | | | | |
| All neighborhoods | 49 | 6–64 | 25 | 24–9934 | 642 | 0.05–1.87 | 0.83 | 17.1–72.6 | 56.0 |
| Mona Ridge | 7 | 7–51 | 18 | 51–155 | 91 | 0.23–0.77 | 0.51 | 35.0–72.6 | 49.8 |
| Lofoten Basin | 4 | 6–28 | 17 | 78–286 | 182 | 0.49–0.69 | 0.58 | 65.2–72.6 | 68.5 |
| Knipovich Ridge | 7 | 14–37 | 27 | 186–751 | 552 | 0.52–1.32 | 0.96 | 60.1–71.2 | 66.1 |
| Western Svalbard shelf | 6 | 15–35 | 27 | 186–9934 | 2920 | 0.58–1.66 | 0.88 | 35.3–71.2 | 54.1 |
| Quaytol chute | 5 | 7–59 | 23 | 24–660 | 170 | 0.47–0.80 | 0.63 | 34.1–61.0 | 47.2 |
| Meridional r-z at 27.5° E. | 6 | 28–53 | 40 | 183–867 | 472 | 1.31–1.87 | 1.70 | 50.0–76.2 | 64.3 |
| Meridional r-z 33° E. | 14 | 10–64 | 23 | 37–254 | 109 | 0.05–1.51 | 0.52 | 17.1–68.2 | 64.3 |
| July-August 2020 г. | | | | | | | | | |
| All neighborhoods | 21 | 3–186 | 45 | 23–1697 | 311 | 0.30–1.56 | 0.92 | 22.2–72.9 | 58.6 |
| Mona Ridge | 7 | 3–27 | 14 | 42–65 | 50 | 0.30–0.51 | 0.44 | 38.5–61.5 | 49.9 |
| Sturfjord | 4 | 36–186 | 90 | 23–830 | 235 | 0.69–1.36 | 1.12 | 22.2–66.2 | 46.3 |
| East Svalbard shelf | 5 | 17–86 | 52 | 57–1697 | 780 | 1.07–1.56 | 1.29 | 59.5–72.9 | 69.6 |
| FJL shelf*** | 5 | 17–30 | 25 | 78–757 | 178 | 0.68–0.87 | 0.83 | 67.6–69.6 | 68.6 |

*Note*. * *n* – Number of samples. ** Results obtained by fluorescence method. *** FJL – Franz Josef Land.

**Table 2.** Distribution of main markers in the composition of bottom sediment alkanes at individual stations

| Horizon | HC, μg/g | Alkanes, μg/g | Alkanes, % of AAU | L/H* | CPI | $\frac{i\text{-}C_{19}}{i\text{-}C_{20}}$ | Paq | Dominant peaks |
|---|---|---|---|---|---|---|---|---|
| Station 7044 | | | | | | | | |
| 0–1 | 26 | 0.1 | 0.56 | 0.87 | 2.38 | 1.73 | 0.43 | $C_{17}$, $C_{19}$, Odd. $C_{21}$–$C_{31}$ |
| Station 7046 | | | | | | | | |
| 0–1 | 15 | 0.1 | 0.53 | 1.07 | 1.67 | 0.19 | 0.39 | $C_{19}$, $C_{29}$, $C_{31}$ |
| 3–4 | 47 | 0.01 | 0.03 | 0.87 | 2.74 | 0.32 | 0.35 | $C_{19}$, $C_{21}$, $C_{29}$, $C_{31}$ |
| 12–14 | 25 | 0.05 | 0.19 | 0.75 | 1.84 | 0.30 | 0.34 | $C_{19}$, $C_{29}$, $C_{31}$ |
| 16–18 | 49 | 0.1 | 0.16 | 0.57 | 4.47 | 0.06 | 0.38 | Nechet. $C_{23}$–$C_{31}$ |
| Station 7063 | | | | | | | | |
| 0–1 | 49 | 0.2 | 0.43 | 0.95 | 1.39 | 0.53 | 0.53 | $C_{19}$, $C_{21}$, $C_{23}$, $C_{25}$ |
| 1–2 | 39 | 0.3 | 0.80 | 1.18 | 1.37 | 0.46 | 0.61 | $C_{19}$, $C_{21}$, $C_{23}$, $C_{25}$ |
| 6–7 | 42 | 0.1 | 0.16 | 1.37 | 1.20 | 0.10 | 0.60 | $C_{19}$, $C_{21}$, $C_{23}$, $C_{25}$ |
| 10–11 | 82 | 0.3 | 0.35 | 1.34 | 1.20 | 0.46 | 0.57 | $C_{17}$, $C_{19}$, $C_{21}$ |
| 14–15 | 71 | 0.3 | 0.40 | 1.54 | 1.38 | 0.48 | 0.59 | $C_{17}$, $C_{19}$, $C_{21}$ |
| 19–20 | 66 | 0.2 | 0.33 | 1.52 | 1.37 | 0.34 | 0.60 | $C_{17}$, $C_{19}$, $C_{21}$ |
| 23–24 | 49 | 0.6 | 1.28 | 1.85 | 1.47 | 0.85 | 0.57 | $C_{17}$, $C_{19}$, $C_{21}$ |
| Station 7064 | | | | | | | | |
| 0–1 | 33 | 0.3 | 0.85 | 1.08 | 1.29 | 1.06 | 0.59 | $C_{17}$, $C_{19}$, Odd. $C_{21}$–$C_{29}$ |
| Station 7066 | | | | | | | | |
| 0–1 | 61 | 0.1 | 0.20 | 4.97 | 1.54 | 9.28 | 0.54 | $C_{15}$, $C_{16}$ |
| Station 7069 | | | | | | | | |
| 0–1 | 49 | 0.4 | 0.84 | 1.09 | 2.13 | 2.40 | 0.45 | $C_{19}$, $C_{25}$–$C_{31}$ |
| 4–5 | 66 | 0.5 | 0.78 | 1.01 | 2.23 | 0.89 | 0.45 | $C_{19}$, $C_{25}$–$C_{31}$ |
| 10–11 | 76 | 0.4 | 0.47 | 1.16 | 2.72 | 1.48 | 0.43 | $C_{19}$, $C_{25}$–$C_{31}$ |
| Station 7083 | | | | | | | | |
| 0–1 | 155 | 3.9 | 2.50 | 0.37 | 6.47 | 0.99 | 0.15 | $C_{29}$, $C_{31}$, $C_{33}$ |
| Station 7085 | | | | | | | | |
| 0–1 | 182 | 0.1 | 0.06 | 2.02 | 4.10 | 0.49 | 0.47 | $C_{15}$, $C_{16}$ |
| Station 7094 | | | | | | | | |
| 0–1 | 21 | 0.2 | 0.75 | 2.04 | 2.60 | 0.31 | 0.56 | $C_{19}$, $C_{20}$ |
| 1–2 | 52 | 0.2 | 0.37 | 1.29 | 2.78 | 0.85 | 0.49 | $C_{19}$, $C_{20}$, Odd. $C_{25}$–$C_{31}$ |
| 7–8 | 87 | 0.1 | 0.10 | 1.45 | 2.71 | 5.93 | 0.43 | $C_{18}$, $C_{20}$ |
| 14–15 | 72 | 0.1 | 0.14 | 1.76 | 2.93 | 2.90 | 0.44 | $C_{18}$, $C_{20}$ |
| 19–20 | 47 | 0.4 | 0.87 | 1.19 | 2.37 | 1.54 | 0.50 | $C_{19}$, Odds. $C_{23}$–$C_{31}$ |
| 31–32 | 42 | 0.1 | 0.36 | 1.73 | 2.35 | 1.78 | 0.80 | $C_{19}$, Odds. $C_{23}$–$C_{31}$ |
| Station 7102 | | | | | | | | |
| 0–1 | 46 | 0.4 | 0.9 | 1.39 | 2.05 | 1.44 | 0.55 | $C_{17}$, $C_{19}$, Odd. $C_{23}$–$C_{31}$ |
| 1–2 | 48 | 0.2 | 0.4 | 1.37 | 2.12 | 1.02 | 0.54 | $C_{17}$, $C_{19}$, Odd. $C_{23}$–$C_{31}$ |
| 2–3 | 48 | 0.3 | 0.6 | 1.24 | 2.20 | 1.47 | 0.55 | $C_{17}$, $C_{19}$, Odd. $C_{23}$–$C_{31}$ |
| 3–4 | 47 | 0.2 | 0.5 | 0.88 | 1.73 | 0.72 | 0.44 | $C_{17}$, $C_{19}$, Odd. $C_{25}$–$C_{31}$ |

**Table 2.** Continued

| Horizon | HC, μg/g | Alkanes, μg/g | Alkanes, % of AAU | L/H* | CPI | $\frac{i\text{-}C_{19}}{i\text{-}C_{20}}$ | Paq | Dominant peaks |
|---|---|---|---|---|---|---|---|---|
| 4–5 | 43 | 0.1 | 0.2 | 1.29 | 2.03 | 1.36 | 0.54 | $C_{17}$, $C_{20}$, Odd. $C_{25}$–$C_{31}$ |
| 5–6 | 36 | 0.2 | 0.7 | 1.14 | 1.84 | 0.81 | 0.57 | $C_{17}$, $C_{19}$, Odd. $C_{23}$–$C_{31}$ |
| 6–7 | 28 | 0.1 | 0.4 | 3.39 | 2.79 | 0.77 | 0.69 | $C_{19}$, $C_{20}$ |
| 7–8 | 39 | 0.2 | 0.5 | 1.45 | 1.94 | 0.28 | 0.58 | $C_{19}$, $C_{20}$, Odd. $C_{25}$–$C_{31}$ |
| 8–9 | 39 | 0.2 | 0.5 | 1.52 | 1.88 | 1.20 | 0.62 | $C_{19}$, $C_{20}$, Odd. $C_{25}$–$C_{31}$ |
| 9–10 | 30 | 0.1 | 0.2 | 1.51 | 1.79 | 1.11 | 0.57 | $C_{20}$ |
| 10–11 | 29 | 0.2 | 0.6 | 1.66 | 2.42 | 0.82 | 0.53 | $C_{17}$, $C_{19}$ |
| 11–12 | 29 | 0.1 | 0.5 | 1.46 | 2.21 | 1.33 | 0.54 | $C_{17}$, $C_{19}$ |
| 12–13 | 28 | 0.2 | 0.7 | 1.58 | 2.09 | 0.67 | 0.56 | $C_{17}$ |
| 13–14 | 29 | 0.2 | 0.7 | 1.41 | 2.09 | 2.74 | 0.56 | $C_{17}$ |
| 14–15 | 24 | 0.2 | 0.6 | 1.15 | 2.08 | 4.34 | 0.53 | $C_{17}$ |
| 15–16 | 24 | 0.2 | 0.6 | 1.30 | 2.05 | 4.03 | 0.53 | $C_{17}$, $C_{19}$ |
| 16–17 | 21 | 0.0 | 0.1 | 1.32 | 1.85 | 2.26 | 0.52 | $C_{17}$, $C_{19}$ |
| 17–18 | 35 | 0.3 | 0.8 | 1.20 | 1.92 | 4.79 | 0.54 | $C_{17}$, $C_{19}$ |
| 18–19 | 29 | 0.1 | 0.5 | 1.25 | 2.09 | 1.75 | 0.49 | $C_{17}$, $C_{19}$, Odd. $C_{25}$–$C_{31}$ |
| 19–20 | 29 | 0.2 | 0.6 | 0.97 | 2.01 | 1.08 | 0.45 | $C_{17}$, $C_{19}$, Odd. $C_{25}$–$C_{31}$ |
| 20–21 | 20 | 0.1 | 0.6 | 1.25 | 2.31 | 1.88 | 0.52 | $C_{17}$, $C_{19}$, Odd. $C_{25}$–$C_{31}$ |
| 21–22 | 19 | 0.2 | 0.9 | 1.20 | 2.09 | 3.73 | 0.52 | $C_{17}$, $C_{19}$, Odd. $C_{25}$–$C_{31}$ |
| 22–23 | 32 | 0.2 | 0.6 | 1.04 | 2.01 | 0.89 | 0.52 | $C_{17}$, $C_{19}$, Odd. $C_{25}$–$C_{31}$ |
| 23–24 | 25 | 0.1 | 0.6 | 1.02 | 1.57 | 1.70 | 0.57 | $C_{17}$, $C_{19}$, Odd. $C_{25}$–$C_{31}$ |
| 24–25 | 28 | 0.2 | 0.7 | 1.00 | 1.88 | 1.39 | 0.52 | Nechet. $C_{23}$–$C_{31}$ |
| 25–26 | 23 | 0.2 | 0.8 | 1.57 | 1.76 | 9.99 | 0.52 | $C_{15}$ |
| 26–27 | 31 | 0.1 | 0.5 | 0.98 | 2.03 | 0.74 | 0.48 | Nechet. $C_{23}$–$C_{31}$ |
| 27–28 | 25 | 0.2 | 0.6 | 1.07 | 2.36 | 3.20 | 0.47 | $C_{17}$, $C_{19}$, Odd. $C_{25}$–$C_{31}$ |
| 28–29 | 27 | 0.2 | 0.7 | 1.01 | 1.88 | 34.94 | 0.48 | $C_{17}$, $C_{19}$, Odd. $C_{25}$–$C_{31}$ |
| 29–30 | 33 | 0.1 | 0.3 | 1.03 | 2.01 | 0.63 | 0.48 | $C_{17}$, $C_{19}$, Odd. $C_{25}$–$C_{31}$ |
| 30–31 | 22 | 0.2 | 0.8 | 1.08 | 1.96 | 6.12 | 0.49 | $C_{17}$, $C_{19}$, Odd. $C_{25}$–$C_{31}$ |
| Station 7104 | | | | | | | | |
| 0–1 | 45 | 0.2 | 0.36 | 1.44 | 2.00 | 0.21 | 0.50 | $C_{17}$ |
| Station 7105 | | | | | | | | |
| 0–1 | 23 | 0.1 | 0.37 | 0.71 | 2.13 | 2.05 | 0.47 | $C_{17}$, $C_{19}$, Odd. $C_{25}$–$C_{31}$ |
| 1–2 | 28 | 0.1 | 0.35 | 0.75 | 1.49 | 12.98 | 0.53 | $C_{17}$, $C_{19}$, Odd. $C_{25}$–$C_{31}$ |
| 2–3 | 33 | 0.1 | 0.18 | 0.76 | 2.07 | 0.30 | 0.49 | $C_{17}$, $C_{19}$, Odd. $C_{25}$–$C_{31}$ |
| 3–4 | 25 | 0.2 | 0.76 | 0.29 | 0.81 | 4.63 | 0.31 | Nechet. $C_{27}$–$C_{31}$ |
| 4–5 | 21 | 0.1 | 0.56 | 1.13 | 2.27 | 1.12 | 0.48 | $C_{19}$ |
| 5–6 | 21 | 0.1 | 0.35 | 0.60 | 3.39 | 1.02 | 0.41 | Odds. $C_{25}$–$C_{31}$ |
| 6–7 | 17 | 0.1 | 0.37 | 0.85 | 2.86 | 4.10 | 0.42 | $C_{15}$, $C_{17}$, $C_{19}$, Odd. $C_{25}$–$C_{31}$ |
| 7–8 | 19 | 0.1 | 0.37 | 0.52 | 2.28 | 1.21 | 0.33 | $C_{19}$, Odds. $C_{25}$–$C_{31}$ |
| 8–9 | 20 | 0.1 | 0.43 | 0.54 | 2.71 | 4.34 | 0.37 | $C_{15}$, $C_{17}$, $C_{19}$, Odd. $C_{25}$–$C_{31}$ |
| 9–10 | 14 | 0.04 | 0.27 | 0.68 | 3.54 | 3.46 | 0.36 | $C_{19}$, Odds. $C_{25}$–$C_{31}$ |

**Table 2.** The End

| Horizon | HC, μg/g | Alkanes, μg/g | Alkanes, % of AAU | L/H* | CPI | $\frac{\text{i-C}_{19}}{\text{i-C}_{20}}$ | Paq | Dominant peaks |
|---|---|---|---|---|---|---|---|---|
| 10–11 | 16 | 0.1 | 0.53 | 0.65 | 2.66 | 15.80 | 0.39 | $C_{19}$, Odds. $C_{25}$–$C_{31}$ |
| 11–12 | 16 | 0.1 | 0.58 | 0.57 | 2.86 | 1.34 | 0.37 | $C_{19}$, Odds. $C_{25}$–$C_{31}$ |
| 12–13 | 17 | 0.1 | 0.59 | 0.53 | 2.85 | 1.62 | 0.37 | Odds. $C_{25}$–$C_{31}$ |
| 13–14 | 17 | 0.1 | 0.53 | 0.59 | 3.85 | 3.23 | 0.35 | Odds. $C_{25}$–$C_{31}$ |
| 14–15 | 15 | 0.1 | 0.62 | 0.53 | 2.99 | 0.92 | 0.37 | Odds. $C_{25}$–$C_{31}$ |
| 15–16 | 19 | 0.1 | 0.38 | 0.92 | 1.96 | 0.71 | 0.45 | $C_{20}$, Odds. $C_{25}$–$C_{31}$ |
| 16–17 | 21 | 0.1 | 0.50 | 0.96 | 1.61 | 1.04 | 0.51 | $C_{15}$ Odds. $C_{25}$–$C_{31}$ |
| 17–18 | 24 | 0.2 | 0.68 | 0.50 | 3.01 | 1.77 | 0.38 | $C_{17}$, Odds. $C_{25}$–$C_{31}$ |
| 18–19 | 19 | 0.1 | 0.67 | 2.25 | 1.92 | 0.13 | 0.48 | $C_{15}$ |
| 19–20 | 20 | 0.1 | 0.31 | 0.60 | 2.33 | 2.90 | 0.43 | $C_{19}$, Odds. $C_{25}$–$C_{31}$ |
| 20–21 | 19 | 0.0 | 0.10 | 0.59 | 2.30 | 2.86 | 0.39 | Odds. $C_{25}$–$C_{31}$ |
| 21–22 | 14 | 0.1 | 0.41 | 0.62 | 3.13 | 0.01 | 0.35 | $C_{17}$, Odds. $C_{25}$–$C_{31}$ |
| 22–23 | 11 | 0.1 | 0.67 | 0.77 | 0.36 | 1.72 | 0.52 | $C_{15}$, Odds. $C_{25}$–$C_{31}$ |
| 23–24 | 13 | 0.2 | 1.27 | 6.34 | 3.40 | 5.33 | 0.47 | $C_{15}$ |
| 24–25 | 14 | 0.1 | 0.50 | 0.61 | 3.02 | 24.42 | 0.41 | $C_{17}$, $C_{19}$, Odd. $C_{25}$–$C_{31}$ |
| 26–27 | 14 | 0.01 | 0.05 | 1.15 | 3.54 | 2.90 | 0.43 | $C_{17}$, $C_{19}$, Odd. $C_{25}$–$C_{31}$ |

* $(L/H - \sum(C_{12-24})/\sum(C_{25-35})$; $CPI - [(C_{25} + C_{27} + C_{29} + C_{31} + C_{33}) / (C_{24} + C_{26} + C_{28} + C_{30} + C_{32}) + (C_{25} + C_{27} + C_{29} + C_{31} + C_{33}) / (C_{26} + C_{28} + C_{30} + C_{32} + C_{34})] / 2$; $Paq - (C_{23} + C_{25})/ (C_{23} + C_{25} + C_{29} + C_{31})$.

part of the column (20–24 cm). At the same time, in the composition of PAHs by hill. 10–11 cm, the number of 2–4 ringed homologs decreased against the background of an increase in 5–6 ringed homologs (Fig. 5), and the ∑light/∑heavy ratio decreased from 1.6 to 1.0 (Table 3).

In the surface layer of sediments at stations 7068 and 7087 sampled in the Lumi and Lunde pockmarks, the content of AHCs was rather low both in terms of dry weight (36–43 μg/g) and $C_{org}$ (0.19–0.26%). A large number of polychaete tubes of the family *Siboglinidae*, as well as hydrocarbon gas escape caverns were observed on the surface and in the sediment column, the number of which increased with sediment depth. The composition of alkanes was dominated by low-molecular-weight homologs, which is determined by their formation, as well as methane [4], in the sediment column.

For surface sediments of the Sofia Basin in the Arctic Ocean, the concentrations of AHCs were even lower: 24–30 μg/g (Fig. 1). Nevertheless, in the oxidized silty-pelitic silt of dark brown color at station 7078, the content of both AHCs (62 μg/g) and PAHs (1222 ng/g) increased. However, in the $C_{org}$ composition, the fraction of AH in this area did not exceed 0.39%.

The HC content increased in the north of the Barents Sea in the Orli and Erik-Eriksen troughs (Fig. 1): for AHCs up to 73 μg/g (station 7100), and for PAHs up to 1125 ng/g (station 7101). Numerous signs of neotectonic activity were identified on acoustic sections in this area [6].

The highest PAHS content (1848–1918 ng/g), against the background of relatively low concentrations of AHCs (21–63 μg/g), is confined to the Svalbard shelf (stations 7059, 7069, 7090, 7091, 7094, 7095). This anomaly was noted earlier [9, 18, 23–25, 28, 31]. The composition of PAHs was dominated by naphthalene and its homologs formed in the sedimentary strata, as their amount practically did not change with the burial depth (Fig. 5, station 7094).

An unusual HC distribution in the sediment column (31 cm column) was found at station 7102, located in the north of the Barents Sea east of Bely Island at the crossing of the Erik-Eriksen Trough (Fig. 1). White Island at the crossing of the Erik-Eriksen Trough (Fig. 1). Here in the aleurite-pelitic bioturbated sludge, the $C_{org}$ content decreased unevenly with burial depth from 2.65 to 2.0%, averaging 2.24%, as did the AHCs – 22–47 μg/g, averaging 31 μg/g (Fig. 5). In the composition of alkanes at transition from oxidized to reduced sediment and change in Eh from

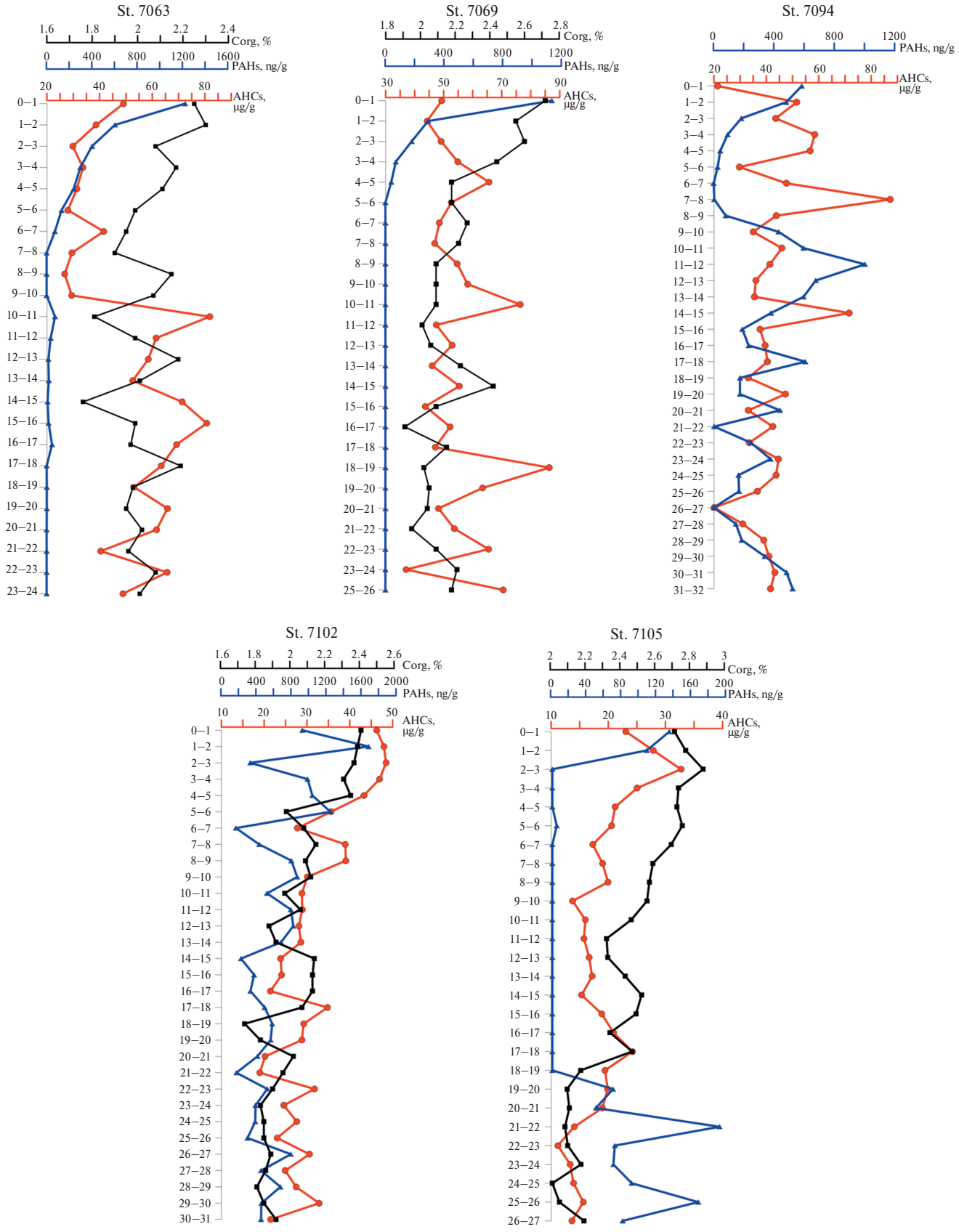


**Fig. 3.** Variation of organic compound concentrations in the sedimentary column of selected stations (station locations are given in Fig. 1).

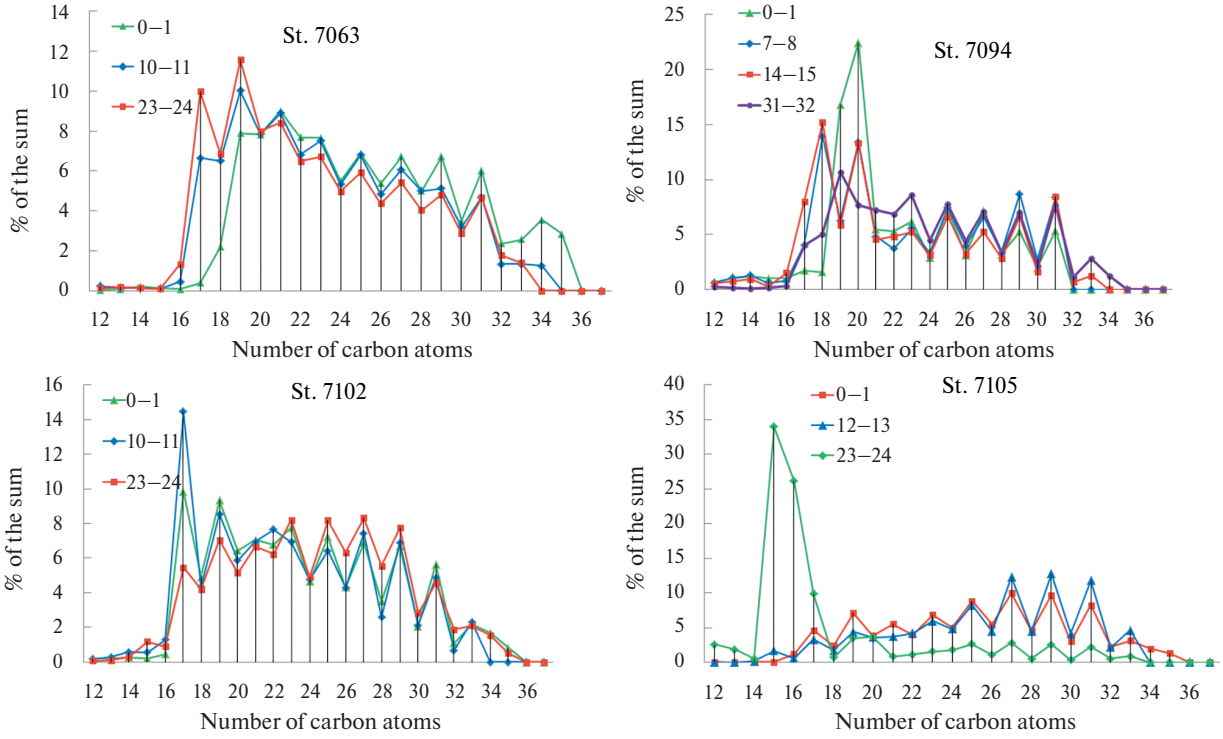


**Fig. 4.** Composition of alkanes in the sedimentary column of selected stations (station locations are given in Fig. 1).

175 (0–1 cm horizon) to -137 (10–11 cm horizon) the formation of autochthonous homolog n-C17 occurred (Fig. 4), and the C17/C25 ratio (2.25) increased 4.7 times compared to the 9–10 cm horizon.

The content of PAHs at station 7102 decreased 2-fold in the sediment thickness: from 931 to 459 ng/g. However, their concentration sharply increased at the transition from the surface oxidized layer to the underlying reduced layer (1–2 cm, up to 1690 ng/g, Fig. 5, Table 3). In contrast to St. 7063, naphthalenes were not among the dominant homologs here (Fig. 5). The PAHS composition was dominated by phenanthrene, the most stable and widespread polyarene in bottom sediments [7, 14, 18, 41].

An anomalous distribution of PAHS concentrations that increased in the lower horizons of the column (Fig. 3) and dominated by 2-methylnaphthalene (Fig. 5), a marker of petroleum genesis [14, 16, 18], was found in the sediments of station 7105 located in the eastern part of the Medvezhinsky Trough [8]. 7105 located in the eastern part of the Medvezhinsky Trough [8]. Sediments at this station were characterized by rather high concentrations of $C_{org}$ in both the surface (2.71%) and lower (2.19%, 25–26 cm) horizons (Fig. 3). In contrast, the content of AHCs was rather low, and their values decreased irregularly from 23 μg/g in the surface layer to 14 μg/g in the lower layer. Nevertheless, autochthonous alkanes occurred in the composition of alkanes in the lower horizons of the column (Fig. 4) and the L/H ratio (Table 2) at the 26–27 cm horizon was almost 2 times higher (1.21) than at the 24–25 cm horizon (0.61). All this indicates natural HC formation in the sedimentary strata. In addition, the formation of PAHs (Fig. 3) occurred in the lower horizons of the core, in the composition of which the share of naphthalenes increased (Fig. 5).

The sediment at station 7044, located in the crater at the site of a volley methane release as a result of dissociation of gas hydrates in the sedimentary strata in the postglacial time, contained a large number of polychaetes and their tubes, as well as shale rubble and driftwood [10]. Such structures are very characteristic of Arctic sea floor topography and are related to the fact that during glaciations, methane from the subsurface reservoir was concentrated in massive mounds beneath the ice sheet [19]. When glaciations retreated, the methane was abruptly released, forming explosive craters. Here, the surface sediment layer (Fig. 1) was characterized by a rather high $C_{org}$ concentration (2.65%), a relatively low AHCs content (26 μg/g), and an elevated PAHS concentration (937 ng/g). Nevertheless, the composition of alkanes in the low molecular weight region showed peaks characteristic of phytoplanktonogenic OM (Fig. 2), and phytane dominated over pristane ($i–C_{19}$ / $i–C_{20}$ = 1.73,

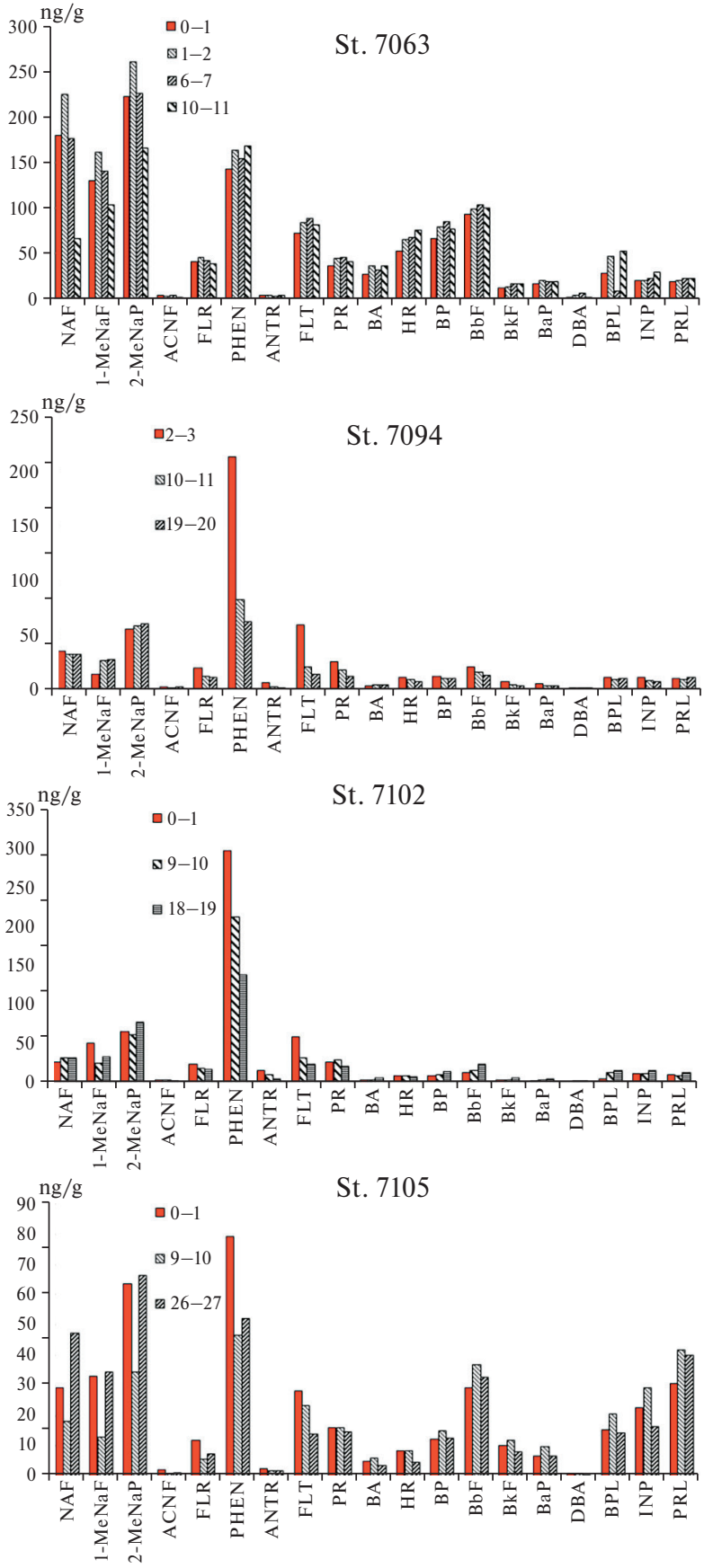


**Fig. 5.** PAHS composition in the sedimentary column of selected stations (station locations are given in Fig. 1).

**Table 3.** Distribution of markers within PAHs (HPLC method) of bottom sediments at some stations

| Horizon | AHCs, μg/g | ∑PAU, ng/g | ∑Naf/ ∑PAHs,% | FLT/PR | ∑Nuff/ PHEN | (PR+FLT)/ (PHEN+ XP) | FEN/. ANTR | ∑2–3 col./ ∑ 5–6 col. | FLT/. (FLT + PR) |
|---|---|---|---|---|---|---|---|---|---|
| Station 7044 | | | | | | | | | |
| 0–1 | 26 | 681 | 30.8 | 1.7 | 1.7 | 0.4 | 25.3 | 1.2 | 0.6 |
| Station 7046 | | | | | | | | | |
| 0–1 | 15 | 81 | 29.6 | 1.8 | 1.5 | 0.4 | 25.8 | 1.1 | 0.6 |
| 2–3 | 78 | 90 | 44.1 | 2.2 | 2.4 | 0.3 | 32.6 | 2.0 | 0.7 |
| 3–4 | 47 | 70 | 58.1 | 4.3 | 3.5 | 0.3 | 39.3 | 3.9 | 0.8 |
| 16–18 | 49 | 466 | 52.5 | 0.9 | 7.3 | 0.4 | 33.8 | 1.6 | 0.5 |
| Station 7063 | | | | | | | | | |
| 0–1 | 49 | 1170 | 45.7 | 2.0 | 3.7 | 0.6 | 39.5 | 1.6 | 0.7 |
| 1–2 | 39 | 1400 | 46.3 | 1.9 | 3.9 | 0.6 | 42.1 | 1.6 | 0.7 |
| 6–7 | 42 | 1270 | 42.9 | 2.0 | 3.5 | 0.6 | 47.0 | 1.4 | 0.7 |
| 10–11 | 82 | 1100 | 30.5 | 2.0 | 2.0 | 0.5 | 42.2 | 1.0 | 0.7 |
| Station 7069 | | | | | | | | | |
| 0–1 | 49 | 450 | 23.5 | 2.2 | 0.9 | 0.5 | 36.1 | 1.2 | 0.7 |
| 1–2 | 44 | 517 | 29.0 | 2.6 | 1.4 | 0.5 | 39.0 | 1.2 | 0.7 |
| 4–5 | 66 | 579 | 30.2 | 2.5 | 1.9 | 0.6 | 44.6 | 1.0 | 0.7 |
| 10–11 | 76 | 513 | 27.5 | 2.6 | 1.8 | 0.6 | 44.9 | 0.9 | 0.7 |
| Station 7078 | | | | | | | | | |
| 0–1 | 62 | 1222 | 35.2 | 2.0 | 1.8 | 0.4 | 41.3 | 1.4 | 0.7 |
| Station 7090 | | | | | | | | | |
| 0–1 | 63 | 387 | 37.3 | 1.3 | 2.2 | 0.4 | 31.8 | 1.4 | 0.6 |
| Station 7091 | | | | | | | | | |
| 0–1 | 148 | 626 | 37.6 | 1.1 | 2.5 | 0.4 | 14.1 | 1.4 | 0.5 |
| Station 7092 | | | | | | | | | |
| 0–1 | 24 | 366 | 38.8 | 2.2 | 1.8 | 0.4 | 24.5 | 2.0 | 0.7 |
| 2–3 | 44 | 520 | 19.8 | 2.3 | 0.5 | 0.4 | 38.1 | 1.9 | 0.7 |
| 3–4 | 58 | 505 | 24.2 | 2.1 | 0.6 | 0.3 | 40.8 | 2.5 | 0.7 |
| 6–7 | 48 | 603 | 25.1 | 1.6 | 0.6 | 0.3 | 30.5 | 2.3 | 0.6 |
| Station 7094 | | | | | | | | | |
| 10–11 | 46 | 327 | 35.9 | 1.2 | 1.4 | 0.4 | 34.3 | 1.9 | 0.5 |
| 11–12 | 41 | 353 | 31.8 | 1.2 | 1.0 | 0.3 | 15.0 | 2.5 | 0.5 |
| 14–15 | 72 | 313 | 36.5 | 1.3 | 1.2 | 0.3 | 19.6 | 2.9 | 0.6 |
| 19–20 | 47 | 294 | 40.9 | 1.1 | 1.9 | 0.4 | 34.6 | 2.1 | 0.5 |
| Station 7095 | | | | | | | | | |
| 0–1 | 62 | 441 | 31.5 | 1.5 | 1.3 | 0.3 | 21.6 | 1.6 | 0.6 |
| Station 7099 | | | | | | | | | |
| 0–1 | 70 | 400 | 30.9 | 1.5 | 1.2 | 0.4 | 13.2 | 1.7 | 0.6 |
| Station 7101 | | | | | | | | | |
| 0–1 | 49 | 1125 | 32.7 | 1.2 | 1.2 | 0.3 | 16.8 | 2.0 | 0.5 |

**Table 3.** The End

| Horizon | AHCs, μg/g | ∑PAU, ng/g | ∑Naf/ ∑PAHs,% | FLT/PR | ∑Nuff/ PHEN | (PR+FLT)/ (PHEN+ XP) | FEN/. ANTR | ∑2–3 col./ ∑ 5–6 col. | FLT/. (FLT + PR) |
|---|---|---|---|---|---|---|---|---|---|
| Station 7102 | | | | | | | | | |
| 0–1 | 46 | 625 | 22.8 | 2.3 | 0.5 | 0.3 | 19.4 | 3.4 | 0.7 |
| 6–7 | 28 | 804 | 20.6 | 1.6 | 0.4 | 0.3 | 14.3 | 3.3 | 0.6 |
| 8–9 | 39 | 614 | 23.3 | 1.2 | 0.5 | 0.3 | 16.0 | 2.8 | 0.5 |
| 9–10 | 30 | 502 | 23.6 | 1.1 | 0.6 | 0.3 | 21.7 | 2.6 | 0.5 |
| 18–19 | 29 | 455 | 31.4 | 1.1 | 1.0 | 0.3 | 31.6 | 2.0 | 0.5 |
| Station 7104 | | | | | | | | | |
| 0–1 | 45 | 710 | 32.7 | 1.8 | 1.1 | 0.2 | 18.2 | 2.4 | 0.6 |
| Station 7105 | | | | | | | | | |
| 0–1 | 23 | 406 | 31.0 | 1.8 | 1.6 | 0.5 | 31.8 | 1.2 | 0.6 |
| 1–2 | 28 | 335 | 22.0 | 1.9 | 1.8 | 0.8 | 29.9 | 0.6 | 0.7 |
| 2–3 | 33 | 256 | 21.2 | 1.8 | 1.8 | 0.7 | 30.5 | 0.6 | 0.6 |
| 3–4 | 25 | 317 | 19.2 | 1.7 | 1.6 | 0.8 | 27.0 | 0.5 | 0.6 |
| 4–5 | 21 | 303 | 24.7 | 1.7 | 2.3 | 0.8 | 23.0 | 0.6 | 0.6 |
| 5–6 | 21 | 316 | 16.7 | 1.8 | 1.3 | 0.8 | 25.4 | 0.5 | 0.6 |
| 6–7 | 17 | 331 | 19.5 | 1.7 | 1.6 | 0.9 | 23.5 | 0.5 | 0.6 |
| 7–8 | 19 | 375 | 19.2 | 1.7 | 1.1 | 0.7 | 23.9 | 0.6 | 0.6 |
| 8–9 | 20 | 351 | 19.8 | 1.6 | 1.2 | 0.7 | 21.9 | 0.6 | 0.6 |
| 9–10 | 14 | 342 | 19.3 | 1.5 | 1.4 | 0.7 | 26.0 | 0.5 | 0.6 |
| 10–11 | 16 | 318 | 25.1 | 1.6 | 1.7 | 0.6 | 26.3 | 0.8 | 0.6 |
| 11–12 | 16 | 344 | 21.2 | 1.6 | 1.3 | 0.7 | 30.6 | 0.7 | 0.6 |
| 12–13 | 17 | 296 | 22.4 | 1.4 | 1.7 | 0.7 | 24.8 | 0.6 | 0.6 |
| 13–14 | 17 | 287 | 19.4 | 1.4 | 1.3 | 0.7 | 26.2 | 0.6 | 0.6 |
| 14–15 | 15 | 286 | 19.2 | 1.4 | 1.3 | 0.7 | 30.3 | 0.6 | 0.6 |
| 15–16 | 19 | 299 | 18.5 | 1.5 | 1.5 | 0.8 | 27.9 | 0.5 | 0.6 |
| 16–17 | 21 | 397 | 25.1 | 1.5 | 1.7 | 0.6 | 24.8 | 0.8 | 0.6 |
| 17–18 | 24 | 437 | 27.2 | 1.9 | 1.2 | 0.4 | 28.3 | 1.2 | 0.6 |
| 18–19 | 19 | 203 | 26.3 | 0.8 | 2.0 | 0.6 | 24.2 | 0.7 | 0.5 |
| 19–20 | 20 | 240 | 29.3 | 0.9 | 2.2 | 0.6 | 22.7 | 0.8 | 0.5 |
| 20–21 | 19 | 246 | 35.3 | 0.9 | 2.7 | 0.6 | 21.4 | 1.0 | 0.5 |
| 21–22 | 14 | 294 | 36.2 | 1.0 | 2.8 | 0.6 | 23.7 | 1.1 | 0.5 |
| 22–23 | 11 | 344 | 41.8 | 0.9 | 2.6 | 0.4 | 27.9 | 1.6 | 0.5 |
| 23–24 | 13 | 323 | 36.0 | 0.9 | 2.2 | 0.5 | 26.1 | 1.2 | 0.5 |
| 24–25 | 14 | 349 | 35.8 | 0.7 | 2.8 | 0.5 | 26.5 | 1.1 | 0.4 |
| 25–26 | 16 | 377 | 39.5 | 0.8 | 2.3 | 0.4 | 32.3 | 1.5 | 0.5 |
| 26–27 | 14 | 381 | 39.0 | 0.9 | 2.8 | 0.5 | 27.6 | 1.2 | 0.5 |

Table 2), which may indicate active biogeochemical processes in the sediment [34].

Thus, for the entire data set obtained in 2021, a correlation ($r = 0.52$, $n = 41$) was observed between precipitation moisture, which varied in the range of 31.6–82.4%, and $C_{org}$. It is known that the porosity and moisture content of precipitation, to a certain extent, are determined by its particle size distribution [2]. Sediments with high moisture content (up to 80% or more) are usually formed by fine suspended sediments with a high proportion of biogenic matter (e.g., fragments of dying planktonic organisms). Low moisture values (less than 40%) are characteristic of coarse bottom sediments formed by lithogenic material entering the seas as a result of coastal erosion and slope runoff.

Between AHCs and moisture ($r = 0.24$) and $C_{org}$ and AHCs ($r = 0.22$) these relationships were much weaker. The distribution of HC determines not so much the lithotype of bottom sediments, but the level of primary production in the water area, the contribution of terrigenous OM, and the influence of benthic macro- and microorganisms [21, 22]. Therefore, in many investigated areas there were no relationships in the distribution of $C_{org}$ and AHCs, AHCs and PAHs. Different nature of formation of AHCs (phytoplankton and oil pollution) and PAHS (fuel combustion processes, to a lesser extent oil pollution) lead to the lack of relationship in the distribution of these hydrocarbon classes: $r$(AHCs–PAHs) = –0.23.

In most cores, there is a decrease in $C_{org}$ concentrations in the upper part of the core (10–12 cm) and an insignificant change in the lower horizons. This pattern corresponds to the general trend of organic matter change in Arctic shelf sediments [31] and rather low CPI values in the composition of alkanes (< 3, Table 2) in the studied water areas indicate an increase in the input of biogenic HCs. Their formation occurred directly in the sedimentary strata, which often had a hydrogen sulfide odor due to a large amount of undecomposed organic compounds (stations 7063, 7068, 7087, 7105).

In Fram Strait, such a large range of concentrations is largely due to the peculiarities of the hydrological regime conditions [33, 36, 39]. Two main currents interact here: the warm West Spitsbergen Current and the cold East Greenland Current. Due to these currents, there is an exchange between Arctic and Atlantic water masses [38]. In the Marginal Ice Zone (MIZ), according to data obtained in 2021, phytoplankton productivity increases to 450–650 $mgC \times m^{-2} \times day^{-1}$ [29]. Increased concentrations of nutrients, chlorophyll-a, high level of phytoplankton production in surface waters, as well as high rates of vertical matter flux lead to accumulation of organic compounds in sediments at some bottom areas. The latter leads to mosaicity in the distribution and composition of organic matter in the surface layer. Earlier it was considered that the main source of HC in the bottom sediments of Fram Strait was phytoplankton (ice algae) and biogeochemical processes at the water-bottom boundary [22]. The contribution of HC of terrestrial origin was minimal. However, our studies showed that terrigenous high-molecular-weight alkanes dominated in the sediments at station 7082. Therefore, the CPI values were higher compared to other areas (Table 2).

The study of the differentiation of the molecular composition of PAHs during transport through the Fram Strait allowed us to establish that the more volatile/light polyarenes, which are formed in emissions at low latitudes, are transported long distances in the atmosphere. In contrast, high molecular weight PAHs are deposited predominantly in coastal shelf water areas as a result of gas exchange between the atmosphere and water [27, 41].

The Westnes Ridge is a drift, the southeastern part of which is complicated by numerous hydrocarbon gas outcrops [37, 40, 43]. At the same time, deep fluids migrate in the sediment column and form not only methane but also high-molecular hydrocarbons. Therefore, at station 7063 in the sedimentary stratum there was a correlation between $C_{org}$ distribution and sediment moisture ($r = 0.58$, $n = 25$), and there were no correlations between AHCs distribution and $C_{org}$ ($r = -0.38$). The latter is most likely due to the presence of a source of organic compounds genetically unrelated to suspension and sedimentation processes. This confirms the distribution of molecular markers in the composition of AHCs and PAHs.

Depending on the conditions in oil and gas bearing horizons and geological structures beneath the seafloor, gas-liquid flows of methane and other HCs from sedimentary strata can become active, temporarily cease their activity, or disappear altogether, and then reappear [11, 35]. This can explain the difference in concentrations of AHCs and PAHS in different years of the study in the same area (Table 1).

The origin of HC differed significantly depending on the study area. It turned out that more stable terrigenous alkanes dominated in sediments only in some areas. That is why CPI values of alkane composition were so low (Table 2). The distribution of methane unloading areas reveals an extremely wide and diverse range of sedimentation settings: landscape-morphological, geodynamic, and climatic [1]. The lack of correlation between $C_{org}$ and AHCs concentrations, the increase in the share of AHCs in the composition

of $C_{org}$ with the depth of sediment burial, and the distribution of markers in the composition of alkanes may testify in favor of the deep nature of AHCs [1, 9]. The local character of these processes is indicated by the lateral variability of AHCs concentrations in sediments.

On the Svalbard shelf, the concentration levels and composition of polyarenes are formed by eroded coal rocks of the archipelago [25, 31]. Therefore, the highest concentrations of PAHs are found here.

The depth processes influence the formation of the modern morphostructure and relief of the Eric-Eriksen and Orly troughs [6]. The general picture of the unloadings location reveals an extremely wide and diverse range of settings of their distribution – landscape-morphological, geodynamic and climatic. The latter is confirmed by anomalously high values of heat flux, in particular, in the Orly trogue more than 300 mW/m$^2$. The activity of deep processes is noted in different segments of the trog because of the tectonic nature of these structures. The western part of the Orly Trough is promising in terms of detecting areas of methane outcrops, which was confirmed by a shipboard echo sounder that established a profile with a flare [10]. That is why there were such high concentrations of HCs, especially PAHs, in the sediments here. The uniqueness of sampling in this area was also due to the fact that in the recent past the troughs of the north of the Barents Sea, were inaccessible for research due to the ice cover and difficult ice situation in the short summer season.

In conclusion, it should be emphasized that the study of HC composition and biogeochemical processes in bottom sediments is now becoming an integral part of research to assess the effects of the changing environment and climate in the Arctic on ecosystems.

## CONCLUSION

The HC sources differed significantly for the studied water areas of the Norwegian-Greenland Basin and the Barents Sea with different sedimentation conditions and deep fluid flows from the bottom. Therefore, large ranges of variation in the concentrations of organic compounds in the surface layer of sediments were established, which amounted to 0.25–2.71% for $C_{org}$, 7–182 μg/g for AHCs and 0–1918 ng/g for PAHs.

The obtained correlations between sediment moisture and $C_{org}$ content indicate the joint content of biogenic and lithogenic components. The absence of correlations between the $C_{org}$ content and HC concentration, as well as between the concentrations of AHCs and PAHs indicate the simultaneous presence of different sources that form these organic compounds in sediments.

In Fram Strait, such a large range of concentrations is largely due to the hydrological conditions of the water area. Both microbial and terrigenous alkanes dominated in the composition of AHCs, and high-molecular-weight homologs prevailed in the composition of PAHs.

In many investigated Holocene sediments, the behavior of organic compounds is mainly due to microseepage of natural HCs (Westness Ridge, Orly Trough area, central part of the Barents Sea, etc.). The composition of alkanes and the composition of PAHs indicated intensive deep fluid flows occurring in the sedimentary strata, which in some cases (st. 7105) can lead to the formation of oil films on the sea surface, registered from space using radar satellites.

The composition of specific biomarkers (e.g., st. 7963) reflects lateral and vertical variability of HC sources in the sediment column. In the water areas of pockmarks and sips, enrichment of the uncovered sedimentary strata with light alkanes in the composition of AHCs and naphthalenes in the composition of PAHs was revealed.

## ACKNOWLEDGEMENTS

The authors thank M. D. Kravchishina, A. A. Klyuvitkin – the management team of the 84th cruise of the R/V “Akademik Mstislav Keldysh” and D. F. Budko for organization and sampling of bottom sediments.

## FUNDING

The work was financially supported by the State Order, topic No. FMWE-2024–0020.

## CONFLICT OF INTERESTS

The authors of this paper have no conflict of interests.

## REFERENCES

1. *Belenitskaya G.A.* Fluid direction of lithology: state, objects, tasks // Scientific Notes of Kazan University. 2011. Vol. 153. No. 4. pp. 97–112.
2. *Gavshin V.M., Lapukhov S.V., Saraev S.V.* Geochemistry of lithogenesis under conditions of hydrogen sulfide contamination (Black Sea). Novosibirsk: Nauka, 1988. 194 p.
3. *Kaminsky V.D., Suprunenko O.I., Smirnov A.N. et al.* Current resource status and prospects for the devel-

opment of the mineral resource base of the shelf area of the Russian Arctic // Exploration and protection of subsoil. 2016. No. 9. pp. 136–142.

4. *Kravchishina M.D., Klyuvitkin A.A., Volodin V.D. et al.* System studies of sedimentation in the European Arctic during the 84th cruise of the research vessel "Akademik Mstislav Keldysh"// Oceanology. 2022. Vol. 62. No. 4. pp. 660–663.
5. *Kursheva A.V., Morgunova I.P., Petrova V.I. et al.* Hydrocarbons in littoral sediments and marsh soils of the southwestern coast of the Barents Sea // Geochemistry. 2023. Vol. 68. No. 9. pp. 964–981. DOI: 10.31857/S0016752523090078
6. *Moroz E.A.* Novel tectonics of the north-western margin of the Barents Sea shelf // Monitoring. Science and Technology. Earth Sciences. 2016. No. 4 (29). pp. 6–13.
7. *Nemirovskaya I.A.* Oil in the ocean (pollution and natural flows). Moscow: Nauchn. Mir, 2013. 432 p.
8. *Nemirovskaya I.A., Ivanov A.Yu.* Verification of remote sensing data to determine the nature of hydrocarbons (on the example of the Barents Sea) // DAN. Earth Sciences. 2022. Vol. 507. № 1. pp. 104–109. doi: 10.31857/S2686739722601168.
9. *Nemirovskaya I.A., Khramtsova A.V.* Hydrocarbons in water and in bottom sediments of the Norwegian-Barents Sea basin// Geochemistry. 2023. Vol. 61. No. 2. pp. 173–186. doi**:** 10.31857/S0016752523020073
10. *Novichkova E.A., Matul A.G., Kozina N.V. et al.* Lithological and paleoceanological studies of the Greenland Basin and the continental margin of Svalbard during the 84th cruise of the R/V "Akademik Mstislav Keldysh" in 2021 // Geology of Oceans and Seas. M.: IORAN, 2022. Vol. 4. pp.118–122.
11. *Patin S.A.* Oil and ecology of the continental shelf. MOSCOW: VNIRO. 2017. Vol. 1. 327 p.
12. *Petrova V.I., Batova G.I., Kursheva A.V. et al.* Hydrocarbons in bottom sediments of the Shtokman area – distribution, genesis, time trends // Oil and Gas Geology. Theory and practice. 2015. Vol. 10. No. 3. URL: http://www.ngtp.ru/rub/1/35_2015.pdf
13. *Reshetnikov M.G.* Climate policy in Russia: Science, technology, economics // Problems of forecasting. 2023. No. 6. pp. 6–10.
14. *Rovinsky F.Ya., Teplitskaya T.A., Alekseeva T.A.* Background monitoring of polycyclic aromatic hydrocarbons. L.: Gidrometeoizdat, 1988. 224 p.
15. Handbooks and manuals. IOC/WMO. Paris: UNESCO, 1984. No. 13. 34 p.
16. *Haustov A.P., Redina M.M.* Geochemical markers based on the ratios of PAHS concentrations in oil and oil-contaminated objects // Geochemistry. 2017. No. 1. pp. 57–67.
17. AMAP. Assessment 2007: Chapter 4. Sources, Inputs and Concentrations of Petroleum Hydrocarbons, Polycyclic Aromatic Hydrocarbons, and other Contaminants Related to Oil and Gas Activities in the Arctic. Oslo, 2010. 87 p.
18. AMAP. Assessment 2016: Chemicals of Emerging Arctic Concern. Oslo, 2017. 353 p.
19. *Andreassen K., Hubbard A., Winsborrow M. et al.* Massive blow-out craters formed by hydratecontrolled methane expulsion from the Arctic seafloor // Science. 2017. Vol. 356 (6341).
20. *Bambulyak A., Frantzen B., Rautio R.* Oil transportation from the Russian part of the Barents region. Status Report. The Norwegian Barents Secretariat and Akvaplan-niva: Norway, 2015. 105 p.
21. *Bianchi T.S., Schreiner K.M., Smith R.W. et al.* Redox effects on organic matter storage in coastal sediments during the Holocene: a biomarker/proxy perspective // Annu. Rev. Earth Planet. Sci. 2016. V. 44. P. 295–319.
22. *Birgel D., Stein R., Hefter J.* Aliphatic lipids in recent sediments of the Fram Strait/Yermak Plateau (Arctic Ocean): composition, sources and transport processes // Marine Chemistry. 2004. Vol. 88. No. 3–4. pp. 127–160.
23. *Boitsov S., Klungsøyr J., Jensen H.* Background concentrations of polycyclic aromatic hydrocarbons (PAHs) in deep core sediments from the Norwegian Sea and the Barents Sea: a proposed update of the OSPAR commission background values for these sea areas // Chemosph. 2020. No. 251. pp. 1–12.
24. *Boitsov S., Klungsøyr J., Jensen H.* Background concentrations of polycyclic aromatic hydrocarbons (PAHs) in deep core sediments from the Norwegian Sea and the Barents Sea: a proposed update of the OSPAR commission background values for these sea areas // Chemosph. 2020. No. 251. pp. 1–12.
25. *Dahle S., Savinov V., Klungsøyr J. et al.* Polyaromatic hydrocarbons (PAHs) in the Barents Sea sediments: small changes over the last 10 years // Mar. Biol. Res. 2009. No. 5. pp. 101–108.
26. *Ivanov A.Y., Ivonin D.V., Terleeva N.V. et al.* Oil spills in the Barents Sea: the results of multiyear monitoring with synthetic aperture radar // Mar. Pollut. Bull. 2022. 179. 113677. https://doi.org/10.1016/j.marpolbul.2022.113677.
27. *Keyte I.J., Harrison R.M., Lammel G.* Chemical reactivity and long-range transport potential of polycyclic aromatic hydrocarbons-A review // Chemical Society Reviews, 2013. Vol. 42 (24), pp. 9333–9391. https://doi.org/10.1039/C3CS60147A.
28. *Koltovskaya E.V., Nemirovskaya I.A.* Concentration and composition of polycyclic aromatic hydrocarbons in bottom sediments of the Barents and Norwegian seas // Oceanology. 2023. Vol. 63. M. Suppl. 1. pp. 144–155.
29. *Kudryavtseva E., Kravchishina M., Pautova L. at al.* Sea Ice as a Factor of Primary Production in the European Arctic: Phytoplankton Size Classes and Carbon Fluxes // J. Mar. Mar. Sci. Eng. 2023. Vol. 11. No. 11. 2131. https://doi.org/10.3390/ jmse11112131
30. Monitoring of hazardous substances in the White Sea and Pechora Sea: harmonization with OSPAR's Co-

ordinated Environmental Monitoring Programme (CEMP) Tromsø: Akvaplan-niva, 2011. 71p.

31. *Morgunova .I.P. Petrova V.I., Litvinenko I.V. et al.* Hydrocarbon molecular markers in the Holocene bottom sediments of the Barents Sea as indicators of natural and anthropogenic impacts // Mar. Poll. Bull. 2019. Vol. 149. No. 12. 110587. https://doi.org/10.1016/j.marpolbul.2019.110587
32. *Nishumura M., Baker E.W.* Possible origin of n-alkanes with remarkable even-to-odd predominance in recent marine sediments // Geochim. Cosmochim. Acta. 1986. Vol. 50. No. 2. pp. 299–305.
33. *Olli K., Wexels Riser, Wassmann C. et al.* Seasonal variation in vertical flux of biogenic matter in the marginal ice zone and the central Barents Sea // Journal of Marine Systems. 2002. Vol. 38. No. 1–2. pp. 189–204.
34. *Peters K.E., Walters C.C., Moldowan J.M.* The Biomarker Guide: Biomarkers and isotopes in petroleum systems and Earth history. Vol.2. Cambridge: Cambridge University Press, 2005. 1155 p.
35. *Rise L., Bellec V.K., Chand S. et al.* Pockmarks in the southwestern Barents Sea and Finnmark fjords // Norwegian Journal of Geology. 2015. Vol. 94. pp. 263–282.
36. *Rudels B., Meyer, R., Fahrbach E. et al.* Water mass distribution in Fram Strait and over the Yermak Plateau in summer 1997 // Ann. Geophys., 2000. Vol. 18. No. 6. pp. 687–705.
37. *Schauer U., Fahrbach E., Osterhus S. et al.* Arctic warming through the Fram Strait: oceanic heat transport from 3 years of measurements // J. Geophys. Geophys. Res. 2004. Vol. 109. p. 06026. doi:10.1029/2003JC001823.
38. *Schneider A., Panieri G., Lepland A. et al.* Methane seepage at Vestnesa Ridge (NW Svalbard) since the Last Glacial Maximum // Quat. Sci. Rev. 2018. Vol. 193. pp. 98–117.
39. *Sztybor K., Rasmussen T.L.* Diagenetic disturbances of marine sedimentary records from methane-influenced environments in the Fram Strait as indications of variation in seep intensity during the last 35,000 years // International Journal of Quaternary research. 2016. Vol. 46. No. 2. pp. 212–228. https://doi.org/10.1111/bor.12202
40. *Sztybor K. Rasmussen T.L.* Late glacial and deglacial palaeoceanographic changes at Vestnesa Ridge, Fram Strait: Methane seep versus non-seep environments // Palaeogeogr. Palaeoclimatol. Palaeoecol. 2017. Vol. 476. pp. 77–89.
41. *Zhang L., Ma Y., Vojta S. et al.* Presence, sources and transport of polycyclic aromatic hydrocarbons in the Arctic Ocean // Geophys. Rev. Lett. 2022. No. 50. GL101496. https://doi.org/10.1029/2022GL101496
42. *Yunker M.W., Macdonald R.W., Ross P.S. et al.* Alkane and PAHS provenance and potential bioavailability in coastal marine sediments subject to a gradient of anthropogenic sources in British Columbia, Canada // Org. Geochem. 2015. No. 89–90. pp. 80–116.
43. *Walczowski W., Piechura J., Osinski R. et al.* The West Spitsbergen Current volume and heat transport from synoptic observations in summer // Deep-Sea Res. Part I. 2005. Vol. 52. No. 8. pp. 1374–1391.